Enhanced contractile force generation by artificial skeletal muscle tissues using IGF-I gene-engineered myoblast cells

Sato, Masanori
Department of Chemical Engineering, Faculty of Engineering, Kyushu University

Ito, Akira
Department of Chemical Engineering, Faculty of Engineering, Kyushu University

Kawabe, Yoshinori
Department of Chemical Engineering, Faculty of Engineering, Kyushu University

Nagamori, Eiji
Toyota Central R&D Laboratories Inc.

他

出版情報：Journal of Bioscience and Bioengineering. 112 (3), pp.273-278, 2011-09. Society for Biotechnology, Japan
バージョン：

Enhanced contractile force generation by artificial skeletal muscle tissues using IGF-I gene-engineered myoblast cells

Masanori Sato,[1] Akira Ito,[1] Yoshinori Kawabe,[1] Eiji Nagamori,[2] and Masamichi Kamihira[1]*

Department of Chemical Engineering, Faculty of Engineering, Kyushu University, 744 Motooka, Nishi-ku, Fukuoka 819-0395, Japan,[1] and Toyota Central R&D Laboratories Inc., 41-1 Yokomichi, Nagakute, Aichi 480-1192, Japan[2]

Running title: IGF-I GENE-ENGINEERED SKELETAL MUSCLE TISSUES

Key words: Skeletal muscle; C2C12 cell; Gene transfer; IGF-I; Tissue engineering

---

*Corresponding author. E-mail: kamihira@chem-eng.kyushu-u.ac.jp

Phone: +81-92-802-2743; Fax: +81-92-802-2793

ABSTRACT

The aim of this study was to investigate whether insulin-like growth factor (IGF)-I gene delivery to myoblast cells promotes the contractile force generated by hydrogel-based tissue-engineered skeletal muscles *in vitro*. Two retroviral vectors allowing doxycycline (Dox)-inducible expression of the IGF-I gene were transduced into mouse myoblast C2C12 cells to evaluate the effects of IGF-I gene expression on these cells. IGF-I gene expression stimulated the proliferation of C2C12 cells, and a significant increase in the growth rate was observed for IGF-I-transduced C2C12 cells with Dox addition, designated C2C12/IGF (Dox+) cells. Quantitative morphometric analyses showed that the myotubes induced from C2C12/IGF (Dox+) cells had a larger area and a greater width than control myotubes induced from normal C2C12 cells. Artificial skeletal muscle tissues were prepared from the respective cells using hydrogels composed of type I collagen and Matrigel. Western blot analyses revealed that the C2C12/IGF (Dox+) tissue constructs showed activation of a skeletal muscle hypertrophy marker (Akt) and enhanced expression of muscle-specific markers (myogenin, myosin heavy chain and tropomyosin). Moreover, the creatine kinase activity was increased in the C2C12/IGF (Dox+) tissue constructs. The C2C12/IGF (Dox+) tissue constructs contracted in response to electrical pulses, and generated a significantly higher physical force than the control C2C12 tissue constructs. These findings indicate that IGF-I gene transfer has the potential to yield functional skeletal muscle substitutes that are capable of *in vivo* restoration of the load-bearing function of injured muscle or acting as *in vitro* electrically-controlled bio-actuators.

INTRODUCTION

Skeletal tissue engineering is considered to be a promising approach for the treatment of muscle disorders caused by traumatic injury or disease (1). In addition, if an artificial skeletal muscle can be applied as an actuator, it may exhibit excellent flexibility and high energy conversion efficiency. Therefore, tissue-engineered skeletal muscle constructs have attracted much attention as bio-actuators in recent years (2,3). For these applications, mimicking of the natural skeletal muscle is believed to be crucial for constructing artificial skeletal muscles that are physiologically equivalent to native muscles. A skeletal muscle is composed of multinucleated muscle fibers that are formed after the differentiation and fusion of myoblasts. Although further understanding of the mechanisms regulating the regenerative processes after loss of skeletal muscle is necessary, a mechanism-based methodology for constructing artificial skeletal muscles may be of great importance.

Insulin-like growth factor (IGF)-I, a peptide growth hormone with high sequence similarity to insulin, has a primary role in promoting the growth and differentiation of skeletal muscle (4). *In vivo*, IGF-I serves as an autocrine/paracrine mediator in muscular processes such as muscle regeneration following injury (5), myotube formation in the developing embryo (6) and stretch-induced myofiber hypertrophy (7). Therefore, the effects of IGF-I on myogenic cells include stimulation of myoblast proliferation, myogenic differentiation and myotube hypertrophy.

Tissue-engineered muscle constructs should be designed to efficiently generate muscular power. To construct three-dimensional tissues, hydrogels derived from extracellular matrix (ECM) components, such as collagen type I and Matrigel, have often been employed to provide a force-transmittable microenvironment for skeletal myoblasts (8) because they support a high cell density and unidirectional cell alignment through the application of geometric constraints. Although the effects of IGF-I overexpression have previously been

studied in transgenic mice (9) and cultured myoblast cells including the mouse myoblast cell line C2C12 (10), these earlier studies did not address the effects of IGF-I expression on the contractile properties of tissue-engineered muscle constructs. Functional evaluation of artificial skeletal muscle tissue constructs is extremely important for their practical application. However, very few quantitative analyses have attempted to characterize the contractile properties of tissue-engineered skeletal muscle. In a previous study, we developed an apparatus for measuring the contractile properties of artificial skeletal muscle tissues and demonstrated its usefulness for evaluating the properties of such muscle tissues (11). The aim of the present study was to clarify the effects of IGF-I overexpression on the biochemical and contractile properties of artificial skeletal muscle tissues.

MATERIALS AND METHODS

Cell culture Mouse C2C12 myoblast cells were cultured in Dulbecco's modified Eagle's medium (DMEM) supplemented with 10% fetal bovine serum (FBS), 100 U/ml penicillin G potassium and 0.1 mg/ml streptomycin sulfate. To induce myogenic differentiation, the medium was changed to DMEM supplemented with 2% calf serum for two-dimensional cell culture or 0.4% Ultroser G (a serum substitute; Pall, East Hills, NY, USA) for three-dimensional tissue culture, 100 U/ml penicillin G potassium and 0.1 mg/ml streptomycin sulfate. 293FT cells were used as a retroviral vector producer based on the Moloney murine leukemia virus (MoMLV) and cultured in high-glucose DMEM supplemented with 10% FBS, 0.1 mM MEM non-essential amino acids (100× NEAA; Invitrogen, Carlsbad, CA, USA) and 20 mM 4-(2-hydroxyethyl)piperazine-1-ethanesulfonic acid (HEPES; Dojindo, Kumamoto, Japan) in collagen-coated tissue culture dishes (Asahi Techno Glass, Tokyo, Japan). All the cells were cultured at 37°C in a 5% CO_2 incubator.

Vector construction MoMLV-derived mouse stem cell virus (MSCV)-based retroviral

vectors were used for gene transfer into C2C12 cells. The Tet-On system (Clontech, Mountain View, CA, USA) was incorporated into the retroviral vectors for inducible expression of the IGF-I gene. For retroviral vector production, two plasmids, pQMSCV/EGFP-CMV-rtTA-WPRE and pQMSCV/EGFP-TRE-IGF-WPRE, were constructed. pQMSCV/EGFP-CMV-rtTA-WPRE encoded a constitutive expression cassette for a transactivator (rtTA) that was activated by the addition of doxycycline (Dox), while pQMSCV/EGFP-TRE-IGF-WPRE encoded an expression cassette for IGF-I including a tet-responsive element, such that IGF-I expression was promoted by the activation of rtTA. These plasmids included an enhanced green fluorescent protein (EGFP) gene under the control of viral LTR promoters to evaluate the viral titer. To construct pQMSCV/EGFP-CMV-rtTA-WPRE, a DNA fragment encoding the EGFP gene was amplified from pIRES-EGFP (Clontech) by PCR, and the resulting fragment was ligated into *Eco*RI- and *Xho*I-digested pQMSCV/CMV-VEGF-IRES-EGFP (12) to generate pQMSCV/EGFP. Next, the woodchuck hepatitis virus posttranscriptional regulatory element (WPRE) sequence from pMSCV/GΔAhEpoW (13) was ligated into *Cla*I-digested pQMSCV/EGFP, resulting in pQMSCV/EGFP-WPRE. Thereafter, the cytomegalovirus (CMV) promoter and the rtTA sequences from pTet-On Advanced (Clontech) were ligated into *Xho*I- and *Cla*I-digested pQMSCV/EGFP-WPRE to generate pQMSCV/EGFP-CMV-rtTA-WPRE. For the construction of pQMSCV/EGF-TRE-IGF-WPRE, a tet-responsive promoter from pTRE-Tight (Clontech) was ligated into *Xho*I- and *Cla*I-digested pQMSCV/EGFP-WPRE to generate pQMSCV/EGFP-TRE-WPRE. Subsequently, an IGF-I cDNA fragment from pCMV-SPORT6 (Clone ID 4194295; Open Biosystems, Huntsville, AL, USA) was ligated into *Bam*HI-digested pQMSCV/EGF-TRE-WPRE to generate pQMSCV/EGFP-TRE-IGF-WPRE.

Retroviral vector production and infection Retroviral vectors pseudotyped with the

vesicular stomatitis G protein (VSV-G) were produced by transient transfection of 293FT cells with three plasmid DNAs, comprising a retroviral vector plasmid (pQMSCV/EGFP-CMV-rtTA-WPRE or pQMSCV/EGFP-TRE-IGF-WPRE), pcDNA4-gag/pol and pLP/VSV-G (14), using the lipofection reagent Lipofectamine 2000 (Invitrogen). The culture medium containing viral vector particles was collected, filtered through a 0.45-μm cellulose acetate filter (Advantec, Tokyo, Japan) and used for retroviral infection.

For the retroviral infection, C2C12 cells (2.5×10^5) were seeded into a 100-mm tissue culture dish (Greiner Bio-one, Frickenhausen, Germany) and cultured for 24 h. Subsequently, the medium was replaced with 10 ml of retroviral solution, comprising a 1:1 mixture of two media containing the retroviral vectors encoding the rtTA and inducible IGF-I expression cassettes. The cells were then cultured in the presence of polybrene (8 μg/ml) for 6 h, resulting in the generation of C2C12 cells capable of Dox-inducible IGF-I expression (C2C12/IGF cells). For all of the retroviral infections, the viral titers against C2C12 cells were determined by flow cytometry using a FACSCalibur (BD Biosciences, Franklin Lakes, NJ, USA). All the viral titers were in the range of $0.7 – 1.2 \times 10^7$ IU/ml.

Detection of IGF-I expression For semiquantitative RT-PCR analysis of IGF-I expression, total RNA was extracted from 1×10^6 cells using an RNAiso Plus Kit (TaKaRa, Otsu, Japan), and reverse-transcribed using ReverTra Ace reverse transcriptase (Toyobo, Osaka, Japan). PCR was performed using IGF-I gene-specific primers (forward: 5’-ggagactggagatgtactgtgc-3’; reverse: 5’-tcttcaaatgtacttcctttcctt-3’) or GAPDH gene-specific primers (forward: 5’-ctacccccaatgtgtccgtc-3’; reverse: 5’-gctgttgaagtcgcaggagac-3’). The PCR was initiated using G-Taq DNA polymerase (Cosmo Genetech, Seoul, Korea) at 95°C for 2 min, followed by 30 cycles of amplification (95°C for 20 s, 72°C for 15 s) and a final extension at 72°C for 5 min. The PCR products were subjected to electrophoresis in a 2%

agarose gel, and the DNA fragments were visualized under ultraviolet light after ethidium bromide staining.

To measure IGF-I secretion quantitatively, the culture media were analyzed using a Mouse IGF-I ELISA Kit (R&D Systems, Minneapolis, MN, USA) according to the manufacturer's protocol.

Effects of IGF-I expression on the proliferation of C2C12 cells The effects of IGF-I expression on myoblast cell growth were examined using C2C12/IGF cells cultured in the presence [C2C12/IGF (Dox+) cells] or absence [C2C12/IGF (Dox–) cells] of Dox (1 μg/ml; Sigma-Aldrich, St Louis, MO, USA). Briefly, C2C12/IGF cells (5×10^4) were seeded into the wells of 6-well tissue culture plates (Greiner Bio-one). The medium with or without Dox was changed every day, and serial subculturing of the cells was performed every 2 days. Cell samples were collected periodically, and the numbers of viable cells were measured by the Trypan blue dye exclusion method.

Effects of IGF-I expression on the differentiation of C2C12 cells C2C12/IGF cells (5×10^4) were seeded into the wells of 6-well tissue culture plates at 2 days before the induction of differentiation (day –2). After culture with or without Dox for 2 days in the growth medium, the medium was replaced with the differentiation medium (day 0) and the cells were further cultured with or without Dox for 7 days. The medium with or without Dox was changed every day. On day 7, the cells were washed with phosphate-buffered saline (PBS) and fixed in 4% paraformaldehyde (PFA) for 15 min. The cells were then permeabilized in PBS containing 0.2% Triton X-100 for 15 min, washed three times with PBS and blocked in PBS containing 1% (w/v) bovine serum albumin (BSA) for 30 min. The cells were incubated with a primary antibody against α-actinin (A-7811, monoclonal anti-α-actinin EA-53; Sigma-Aldrich) for 45 min, washed three times with PBS and immersed in PBS containing an Alexa 488-conjugated secondary antibody (Invitrogen) and 1% BSA for 45 min. After three washes, the cells were

observed under a BZ-9000 fluorescence microscope (Keyence, Tokyo, Japan). Microscopic images of five fields in each of three separate wells per sample were captured and saved to a disk for later analysis. The α-actinin-positive myotube area and width were measured using ImageJ software (NIH, Bethesda, MD, USA).

Fabrication of artificial skeletal muscle tissue constructs A collagen solution was prepared by mixing type I collagen (Nitta Gelatin, Osaka, Japan), 5× DMEM, neutralization buffer (0.05 N NaOH) and FBS at a volume ratio of 7:1:1:1. A C2C12 cell suspension (1×10^6 cells in 100 μl) was mixed with an ECM precursor solution composed of 170 μl of collagen solution and 30 μl of Matrigel basement matrix (BD Biosciences). The final concentration of type I collagen was adjusted to 0.5 mg/ml. Subsequently, the mixture (300 μl/well) was placed in the wells of a 24-well ultra-low attachment plate (Corning, New York, NY, USA) that had a polycarbonate cylinder (diameter, 8 mm; height, 9 mm) fixed at the center of each well. The procedure was conducted on ice. The ECM components were hardened by incubation at 37°C for 1 h. Thereafter, the growth medium was added to each well. After culture for 2 days, the cell layer had completely shrunk around the cylinder, resulting in the formation of a ring-shaped bundle. The bundle was removed from the cylinder and hooked around two stainless-steel pins (0.6 mm in diameter; Shiga, Tokyo, Japan) that were positioned 12 mm apart from one another. The bundles were cultured in the differentiation medium for 7 days to induce artificial muscle tissue constructs. The medium was changed every day.

Histological analysis For histological evaluation, the artificial muscle tissue constructs were washed three times with PBS, fixed in 4% PFA in PBS and embedded in paraffin. Thin sections (4 μm) were cut and stained with hematoxylin and eosin (H&E). The stained sections were observed under an IX71 microscope (Olympus, Tokyo, Japan).

Western blot analysis Cellular proteins were extracted from the artificial muscle tissue

constructs by a method involving homogenization and freeze-thawing. Protein samples (30 μg) were mixed with SDS-PAGE sample buffer containing 2-mercaptoethanol and boiled at 100°C for 5 min. Subsequently, the samples were electrophoresed in a 7.5% [for myosin heavy chain (MHC)] or 12% [for Akt, phospho-Akt (p-Akt), myogenin, tropomyosin and GAPDH] acrylamide gel and the separated proteins were transferred to a polyvinylidene fluoride membrane (GE Healthcare, Buckinghamshire, UK). After blocking with 5% skimmed milk in Tris-buffered saline containing 0.05% Tween 20 (TBS-T) at 4°C overnight, the membrane was incubated with a primary antibody [anti-Akt (#9272; Cell Signaling Technology, Danvers, MA, USA), anti-p-Akt (#9271; Cell Signaling Technology), anti-myogenin (ab1835; Abcam, Cambridge, UK), anti-MHC (sc20641; Santa Cruz Biotechnology, Santa Cruz, CA, USA), anti-tropomyosin (ab7785; Abcam) or anti-GAPDH (#2118; Cell Signaling Technology)] for 1 h. The bound antibodies were detected using horseradish peroxidase-conjugated secondary antibodies (Santa Cruz Biotechnology) and a chemiluminescence detection kit (ECL detection system; GE Healthcare).

Creatine kinase activity The artificial muscle tissue constructs were rinsed with PBS and homogenized in a cell lysis buffer comprising 10 mM Tris-HCl (pH 7.2), 1 M NaCl, 1 mM EDTA and 1% Triton X-100 (15). The creatine kinase activity in the samples was determined using a commercially available assay kit (CPK-II Test Wako; Wako Pure Chemical Industries, Tokyo, Japan).

Tension measurement Carbon electrodes were placed 10 mm apart at opposite sides of a tissue culture plate. An artificial tissue ring was hooked around two stainless-steel minutien pins (0.3 mm in diameter; Shiga). One pin was attached to a force transducer (AE-801; SonorOne, Sausalito, CA, USA) and the other was fixed to a silicon rubber sheet placed on the bottom of the culture plate. During testing, the medium was maintained at 30 – 32°C using a heated aluminum platform (HI-1000; AsOne, Osaka, Japan). Electrical pulses were

controlled by a personal computer with specially designed LabView software (National Instruments, Austin, TX, USA), and the applied electrical pulse and measured force were recorded using the same computer. For measuring twitch contractions, the tissue sample was stimulated with an electrical pulse of 20 V with a width of 10 ms. For measuring tetanic contractions, the tissue sample was stimulated with an electrical pulse with the following properties: voltage, 20 V; width, 10 ms; frequency, 50 Hz; duration, 2 s.

Statistical analysis Statistical comparisons were performed using the Mann–Whitney rank sum test. Values of $P < 0.05$ were considered to indicate significant differences.

RESULTS AND DISCUSSION

Generation of C2C12/IGF cells The cell proliferation (mitogenesis) and differentiation (myogenesis) that occur during muscle development are complex processes, and the majority of mitogens stimulate the cell proliferation and inhibit the cell differentiation. Therefore, IGF-I possesses a unique characteristic among growth factors in that it stimulates both cell proliferation and differentiation. To distinguish between the effects on myoblast proliferation and differentiation in the present study, a retroviral vector system allowing inducible expression of IGF-I was designed. The system consisted of a combination of two retroviral vectors, one for constitutively expressing rtTA which can be activated by Dox addition and the other for expressing the IGF-I cDNA under the control of an inducible promoter containing a binding site (TRE) for activated rtTA. Thus, if cells are infected with the two retroviral vectors, IGF-I gene expression is induced in the presence of Dox via rtTA activation. C2C12 cells were infected with the two retroviral vectors to generate C2C12/IGF cells. To investigate the inducible IGF-I expression, C2C12/IGF cells were cultured in the presence or absence of Dox for 2 days and the IGF expression was measured. RT-PCR analyses using mouse IGF-I-specific primers revealed that C2C12/IGF (Dox–) cells as well as parental

C2C12cells (data not shown) expressed endogenous IGF-I at low levels, while C2C12/IGF (Dox+) cells overexpressed IGF-I (Fig. 1A). The IGF-I secretion into the culture medium was determined by ELISA. The secretion levels of C2C12/IGF (Dox–) cells and C2C12/IGF (Dox+) cells were 0.26 ± 0.01 and 6.53 ± 0.15 ng/(ml•day), respectively (Fig. 1B). These results demonstrate that the inducible IGF-I expression system was successfully constructed in C2C12 cells.

Effects of IGF-I expression on the proliferation of C2C12 cells The numbers of C2C12/IGF cells cultured in the growth medium with or without Dox addition were counted every day during a 7-day culture period (Fig. 2). The specific growth rate of C2C12/IGF (Dox+) cells (μ = 1.20 day^{-1}; calculated from Fig. 2) was 1.3 times higher than that of C2C12/IGF (Dox–) cells (μ = 0.94 day^{-1}; calculated from Fig. 2), and the number of C2C12/IGF (Dox+) cells on day 7 was 7.0 times higher than that of C2C12/IGF (Dox–) cells. In our preliminary experiments, normal C2C12 cells cultured in IGF-I-containing medium also showed a proliferative response, suggesting that autocrine/paracrine release of IGF-I from genetically engineered myoblast cells or tissue-engineered constructs may stimulate skeletal muscle growth.

Myotube hypertrophy induction by IGF-I during differentiation To induce myogenic differentiation, C2C12/IGF (Dox+) or C2C12/IGF (Dox–) cells were cultured for 2 days in the growth medium and recultured for 7 days in the differentiation medium. As shown in Fig. 3A, myotube hypertrophy was observed in the C2C12/IGF (Dox+) myotubes based on both the myotube area and width. Quantitative image analyses revealed that the C2C12/IGF (Dox+) myotubes had a larger cell area (25500 ± 1110 μm^2 versus 12200 ± 535 μm^2; P < 0.05) and a greater myotube width (45.5 ± 2.8 μm versus 34.6 ± 4.6 μm; P < 0.05) than normal C2C12 myotubes. Since IGF-I stimulates cell proliferation and differentiation through the mitogen-activated protein kinase (MAPK) and phosphatidylinositol 3-kinase (PI3K)

cascades, respectively (16), we supposed that constitutive expression of IGF-I during the proliferation phase may affect the subsequent myogenic differentiation. Therefore, we investigated whether the hypertrophic response of C2C12/IGF myotubes was influenced by the timing of Dox addition. Interestingly, we found that the timing of Dox addition did not significantly affect the augmentation of the myotube area and width (Fig. 3B). Since the reduced serum concentration in the differentiation medium causes C2C12 myoblasts to exit the cell cycle and fuse into myotubes, we supposed that the effects of the differentiation medium were more responsible for the myogenic differentiation of C2C12 cells than IGF-I overexpression. Although myotube hypertrophy was induced by IGF-I overexpression during differentiation, the timing of IGF-I induction until day 3 after the medium change for differentiation did not affect the myotube hypertrophy. Semsarian et al. (10) also reported that constitutive expression of IGF-I did not affect switching from a proliferation phase to a differentiation phase in C2C12 cells. The signaling mechanism mediated by IGF-I in growth and differentiation of myoblasts remains to be elucidated.

Fabrication of artificial muscle tissue constructs To explore the impact of IGF-I gene transfer on engineered skeletal muscle structure and function, we fabricated C2C12/IGF muscle bundles made of type I collagen and Matrigel. Cell-mediated gel contraction was observed within 1 day (Fig. 4A) and muscle bundles with an average diameter of 643 ± 42 μm were formed. As shown in Fig. 4B, H&E staining revealed that the muscle bundles after 7 days of culture in the differentiation medium consisted of an outer region with densely packed cells and a relatively acellular central core region. The outermost cell layer was composed of longitudinally oriented myotubes. Interestingly, although the densities of normal C2C12, C2C12/IGF (Dox–) and C2C12/IGF (Dox+) cells within the bundles were similar, long myotubes were observed at an inner region within the C2C12/IGF (Dox+) bundles. Since anti-apoptotic activity was reported for IGF-I (17), the enhanced expression of IGF-I might

support cell survival in the inner region of the bundles, resulting in the promotion of myogenic differentiation within the artificial muscle tissue constructs.

Biochemical analysis of the artificial muscle tissue constructs To evaluate the skeletal muscle differentiation, the expression levels of myogenin, MHC and tropomyosin were measured in the artificial tissue constructs by western blot analyses (Fig. 5A). The expression of the early-stage muscle-specific transcription factor myogenin, which plays a crucial role in muscle fusion and myotube formation (18), was enhanced in the C2C12/IGF (Dox+) muscle bundles. Moreover, the expressions of MHC and tropomyosin, as later-stage muscle-specific proteins, were also enhanced. The myogenic differentiation signals induced by IGF-I are mediated by the PI3K/Akt pathway (19). To determine whether these myogenic responses were induced by IGF-I expression, we examined Akt expression in the artificial muscle tissue constructs. We found that the level of phosphorylated Akt (p-Akt) was increased in the C2C12/IGF (Dox+) muscle bundles without altering the total Akt protein level, indicating that IGF-I overexpression induced Akt activation. These results demonstrate that the muscle differentiation of the artificial tissue constructs can be promoted by IGF-I expression. Next, the creatine kinase activity of the artificial tissue constructs was measured, since creatine kinase is involved in the energy metabolism of muscle tissues during muscle contraction (20). As shown in Fig. 5B, the creatine kinase activity was enhanced in the C2C12/IGF (Dox+) muscle bundles.

Contractile properties of the artificial skeletal muscle tissues To evaluate the contractile properties, the artificial skeletal muscle constructs were stimulated with electrical pulses. Twitching responses were elicited using a single electrical pulse (voltage, 20 V; width, 10 ms) while tetanus responses were stimulated by continuous electrical pulses (voltage, 20 V; width, 10 ms; frequency, 50 Hz; duration, 2 s). The force generation profiles in response to the electrical stimulations are shown in Fig. 6A. Similar to natural skeletal muscle tissues, twitch

contractions occurred after low-frequency electrical stimulation, while the additional activation of contractile elements, *i.e.* tetanus, was observed by repeated electrical stimulation with a higher frequency. These results indicate that the properties of the artificial tissue constructs were qualitatively very similar to those of natural skeletal muscle tissues. The maximum contractile forces produced by the muscle bundles on day 7 are shown in Fig. 6B. The C2C12/IGF (Dox+) muscle bundles generated a significantly higher physical force by the twitching (9.4 ± 3.5 μN versus 16.5 ± 2.6 μN; $P < 0.05$) and tetanus (23.2 ± 7.6 μN versus 35.4. ± 5.2 μN; $P < 0.05$) contractions than the C2C12/IGF (Dox–) muscle bundles. The contractile force properties of the artificial tissue constructs were consistent with the creatine kinase activities of the constructs (Fig. 5B). These results indicate that the IGF-I gene transfer into myoblasts improved the cell function after differentiation.

In the present study, the artificial skeletal muscle tissue constructs fabricated by hydrogel-based tissue engineering successfully contracted in response to electrical pulses. As shown in Fig. 6B, the C2C12/IGF (Dox+) tissue constructs generated a maximum twitch force of 19.8 μN, which corresponds to two to three orders of magnitude less than the forces measured in normal adult muscle (21,22). The composition of the ECM that surrounds the embedded muscle cells in tissue-engineered skeletal muscle may be one of the most important determinant factors for the contractile function of artificial skeletal muscle. Since tissue-engineered muscle, unlike native muscle tissue, is generally composed of relatively short myotubes, its force generation and transmission are profoundly influenced by cell-matrix interactions. Recently, Hinds et al. (23) reported that increased hydrogel concentrations of fibrin and Matrigel synergistically augmented the force generation capacity of hydrogel-based tissue constructs using neonatal rat skeletal myoblasts, and the optimal matrix composition (4 mg/ml fibrin with 40% Matrigel) yielded 2.84 mN. In the present study, long myotubes were observed in the C2C12/IGF (Dox+) muscle bundles (Fig. 4B), suggesting

that further manipulation of the hydrogel matrix composition (*i.e.* cell-matrix interactions) may improve the contractile force generation capacity in the IGF-I-transduced artificial muscle tissue constructs.

In conclusion, we have shown that IGF-I gene transfer is a promising approach for improving the contractile function of tissue-engineered muscle tissue, as demonstrated by a 1.7-fold increase in the twitch force amplitude in C2C12/IGF (Dox+) bundles compared with C2C12/IGF (Dox–) bundles. This strategy holds potential for yielding functional skeletal muscle substitutes capable of *in vivo* restoration of the load-bearing function of injured muscle or acting as *in vitro* electrically-controlled bio-actuators.

ACKNOWLEDGMENT

This work was supported in part by a Grant-in-Aid for Scientific Research (no. 21686079) from the Japan Society for the Promotion of Science.

References

1. **Liao, H. and Zhou, G.Q.**: Development and progress of engineering of skeletal muscle tissue. Tissue Eng. Part B Rev., **15**, 319-331 (2009).
2. **Feinberg, A.W., Feigel, A., Shevkoplyas, S.S., Sheehy, S., Whitesides, G.M., and Parker, K.K.**: Muscular thin films for building actuators and powering devices. Science, **317,** 1366-1370 (2007).
3. **Fujita, H., Van Dau, T., Shimizu, K., Hatsuda, R., Sugiyama, S., and Nagamori, E.**: Designing of a Si-MEMS device with an integrated skeletal muscle cell-based bio-actuator. Biomed. Microdevices, **13**, 123-129 (2011).
4. **Cohick, W.S. and Clemmons, D.R.**: The insulin-like growth factors. Annu. Rev. Physiol., **55**, 131-153 (1993).

5. **Takahashi, T., Ishida, K., Itoh, K., Konishi, Y., Yagyu, K.I., Tominaga, A., Miyazaki, J.I., and Yamamoto, H.**: IGF-I gene transfer by electroporation promotes regeneration in a muscle injury model. Gene Ther., **10**, 612-620 (2003).
6. **Han, V.K., D'Ercole, A.J., and Lund, P.K.**: Cellular localization of somatomedin (insulin-like growth factor) messenger RNA in the human fetus. Science, **236**, 193-197 (1987).
7. **DeVol, D.L., Rotwein, P., Sadow, J.L., Novakofski, J., and Bechtel, P.J.**: Activation of insulin-like growth factor gene expression during work-induced skeletal muscle growth. Am. J. Physiol., **259**, E89-E95 (1990).
8. **Giraud, M.N., Ayuni, E., Cook, S., Siepe, M., Carrel, T.P., and Tevaearai, H.T.**: Hydrogel-based engineered skeletal muscle grafts normalize heart function early after myocardial infarction. Artif. Organs., **32**, 692-700 (2008).
9. **Coleman, M.E., DeMayo, F., Yin, K.C., Lee, H.M., Geske, R., Montgomery, C., and Schwartz, R.J.**: Myogenic vector expression of insulin-like growth factor I stimulates muscle cell differentiation and myofiber hypertrophy in transgenic mice. J. Biol. Chem., **270**, 12109-12116 (1995).
10. **Semsarian, C., Sutrave, P., Richmond, D.R., and Graham, R.M.**: Insulin-like growth factor (IGF-I) induces myotube hypertrophy associated with an increase in anaerobic glycolysis in a clonal skeletal-muscle cell model. Biochem. J., **339**, 443-451 (1999).
11. **Yamamoto, Y., Ito, A., Fujita, H., Nagamori, E., Kawabe, Y., and Kamihira, M.**: Functional evaluation of artificial skeletal muscle tissue constructs fabricated by a magnetic force-based tissue engineering technique. Tissue Eng. Part A., **17**, 107-114 (2011).

12. **Akiyama, H., Ito, A., Kawabe, Y., and Kamihira, M.**: Genetically engineered angiogenic cell sheets using magnetic force-based gene delivery and tissue fabrication techniques. Biomaterials, **31**, 1251-1259 (2010).
13. **Penno, C.A., Kawabe, Y., Ito, A., and Kamihira, M.**: Production of recombinant human erythropoietin/Fc fusion protein by genetically manipulated chickens. Transgenic Res., **19**, 187-195 (2010).
14. **Hotta, A., Saito, Y., Kyogoku, K., Kawabe, Y., Nishijima, K., Kamihira, M., and Iijima, S.**: Characterization of transient expression system for retroviral vector production. J. Biosci. Bioeng., **101**, 361-368 (2006).
15. **Yoshiko, Y., Hirao, K., and Maeda, N.**: Differentiation in C2C12 myoblasts depends on the expression of endogenous IGFs and not serum depletion. Am. J. Physiol. Cell Physiol., **283**, C1278-C1286 (2002).
16. **Singleton, J.R. and Feldman, E.L.**: Insulin-like growth factor-I in muscle metabolism and myotherapies. Neurobiol. Dis., **8**, 541-554 (2001).
17. **Napier, J.R., Thomas, M.F., Sharma, M., Hodgkinson, S.C., and Bass, J.J.**: Insulin-like growth factor-I protects myoblasts from apoptosis but requires other factors to stimulate proliferation. J. Endocrinol., **163**, 63-68 (1999).
18. **Hasty, P., Bradley, A., Morris, J.H., Edmondson, D.G., Venuti, J.M., Olson, E.N., and Klein, W.H.**: Muscle deficiency and neonatal death in mice with a targeted mutation in the myogenin gene. Nature, **364**, 501-506 (1993).
19. **Rommel, C., Bodine, S.C., Clarke, B.A., Rossman, R., Nunez, L., Stitt, T.N., Yancopoulos, G.D., and Glass, D.J.**: Mediation of IGF-1-induced skeletal myotube hypertrophy by PI(3)K/Akt/mTOR and PI(3)K/Akt/GSK3 pathways. Nat. Cell Biol., **3**, 1009-1013 (2001).

20. **Bessman, S.P. and Geiger, P.J.**: Transport of energy in muscle: the phosphorylcreatine shuttle. Science, **211**, 448-452 (1981).
21. **Close, R.I.**: Dynamic properties of mammalian skeletal muscles. Physiol. Rev., **52**, 129-197 (1972).
22. **Isaacson, A., Hinkes, M.J., and Taylor, S.R.**: Contracture and twitch potentiation of fast and slow muscles of the rat at 20 and 37°C. Am. J. Physiol., **218**, 33-41 (1970).
23. **Hinds, S., Bian, W., Dennis, R.G., and Bursac, N.**: The role of extracellular matrix composition in structure and function of bioengineered skeletal muscle. Biomaterials, **32**, 3575-3583 (2011).

Figure legends

FIG. 1. Generation and characterization of C2C12/IGF cells. (A) The IGF-I expression in C2C12/IGF cells with or without Dox (Dox+ and Dox–, respectively) was analyzed by semiquantitative RT-PCR. (B) The IGF-I secretion into the culture medium by C2C12/IGF cells with or without Dox (Dox+ and Dox–, respectively) was analyzed by ELISA. The data points are the means ± SD of triplicate experiments. *$P < 0.05$.

FIG. 2. Effects of IGF-I expression on the proliferation of C2C12 cells. The time-dependent increase in the number of C2C12 cells (circles) and C2C12/IGF cells cultured in the presence (triangles) or absence (squares) of Dox were measured. The data points are the means ± SD of triplicate experiments.

FIG. 3. Effects of IGF-I expression on the differentiation of C2C12 cells. (A) Microscopic images of α-actinin-positive myotubes. C2C12/IGF cells were cultured in the presence [C2C12/IGF (Dox+)] or absence [C2C12/IGF (Dox–)] of Dox for 2 days in the growth medium (GM) and subsequently cultured for 7 days in the differentiation medium (DM). The medium with or without Dox was changed every day. (B) Quantitative image analysis of myotube hypertrophy. C2C12/IGF cells were cultured in the presence or absence of Dox for 2 days in GM and subsequently cultured for 7 days in DM. The time schedule for the addition of Dox was varied as shown in (a) and (b). *$P < 0.05$ versus normal C2C12 cells treated with the same protocol.

FIG. 4. Histology of the artificial skeletal muscle tissue constructs. (A) Macroscopic photograph of a ring-shaped muscle bundle cultured around stainless-steel pins after 7 days of

culture in the differentiation medium. The arrowheads indicate a muscle bundle. (B) Bright-field micrographs of H&E-stained sections of muscle bundles constructed using normal C2C12 cells, C2C12/IGF (Dox–) cells or C2C12/IGF (Dox+) cells on day 7. The arrowheads indicate long myotubes at a relatively central region within the C2C12/IGF (Dox+) bundle.

FIG. 5. Biochemical evaluation of the artificial skeletal muscle tissue constructs. (A) Western blot analyses of muscle-specific proteins in artificial tissue constructs. The expressions of myogenin, MHC, tropomyosin, p-Akt, Akt and GAPDH in the muscle bundles were analyzed after 7 days of culture in the differentiation medium. (B) Creatine kinase activity. The data are expressed as the means ± SD of three bundles. *$P < 0.05$ and **$P < 0.05$ versus normal C2C12 bundles and C2C12/IGF (Dox–) bundles, respectively.

FIG. 6. Contractile properties of the artificial skeletal muscle tissue constructs. (A) A representative peak of the twitch force generated by the muscle bundles (*left*) and the fusion of tetanus of the muscle bundles (*right*) after 7 days of culture in the differentiation medium. (B) Maximum twitch (*left*) and tetanus (*right*) forces of the muscle bundles. The data are expressed as the means ± SD of three bundles. *$P < 0.05$ and **$P < 0.05$ versus normal C2C12 bundles and C2C12/IGF (Dox–) bundles, respectively.

A

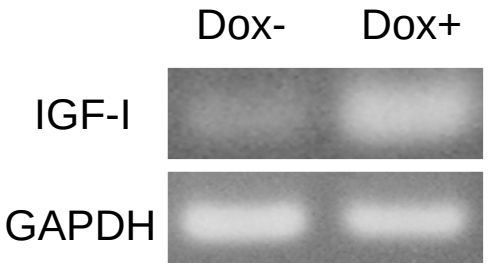

B

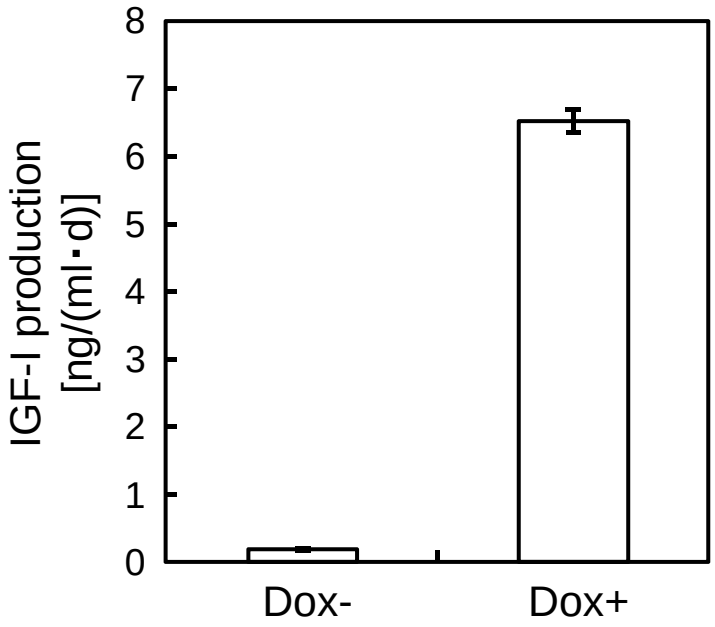

Fig. 1 Sato *et al.*

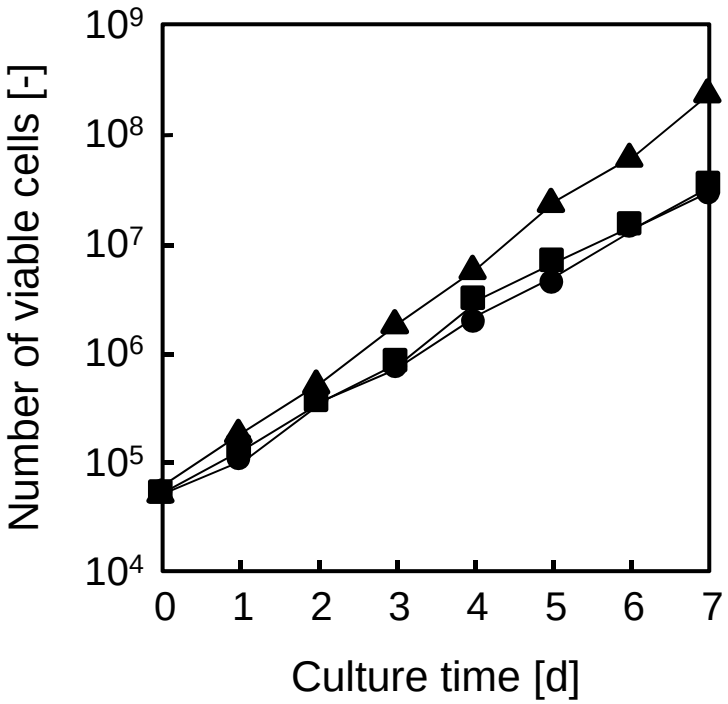

Fig. 2 Sato *et al.*

A

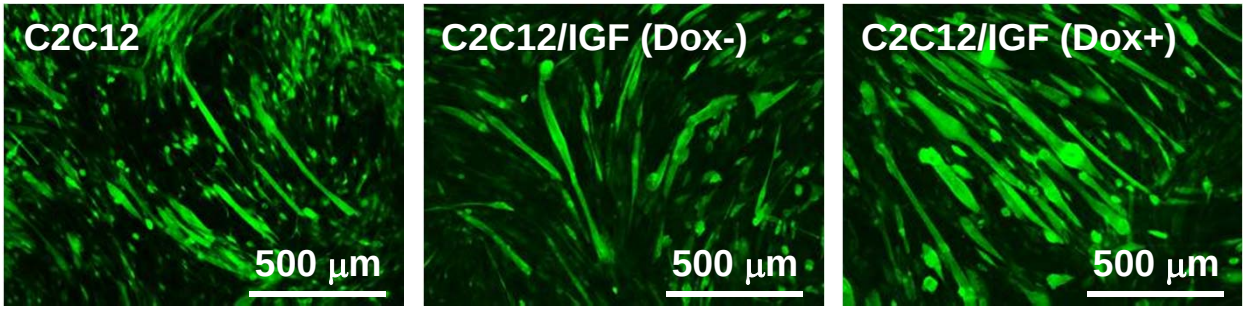

B

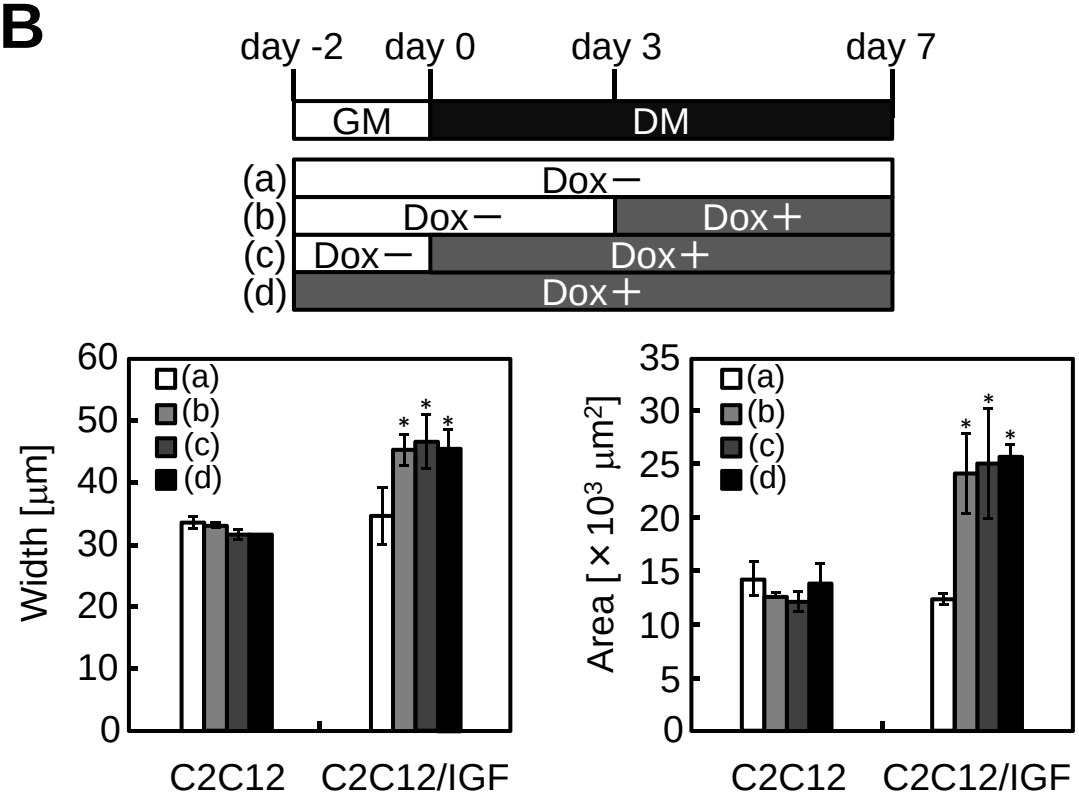

Fig. 3 Sato *et al.*

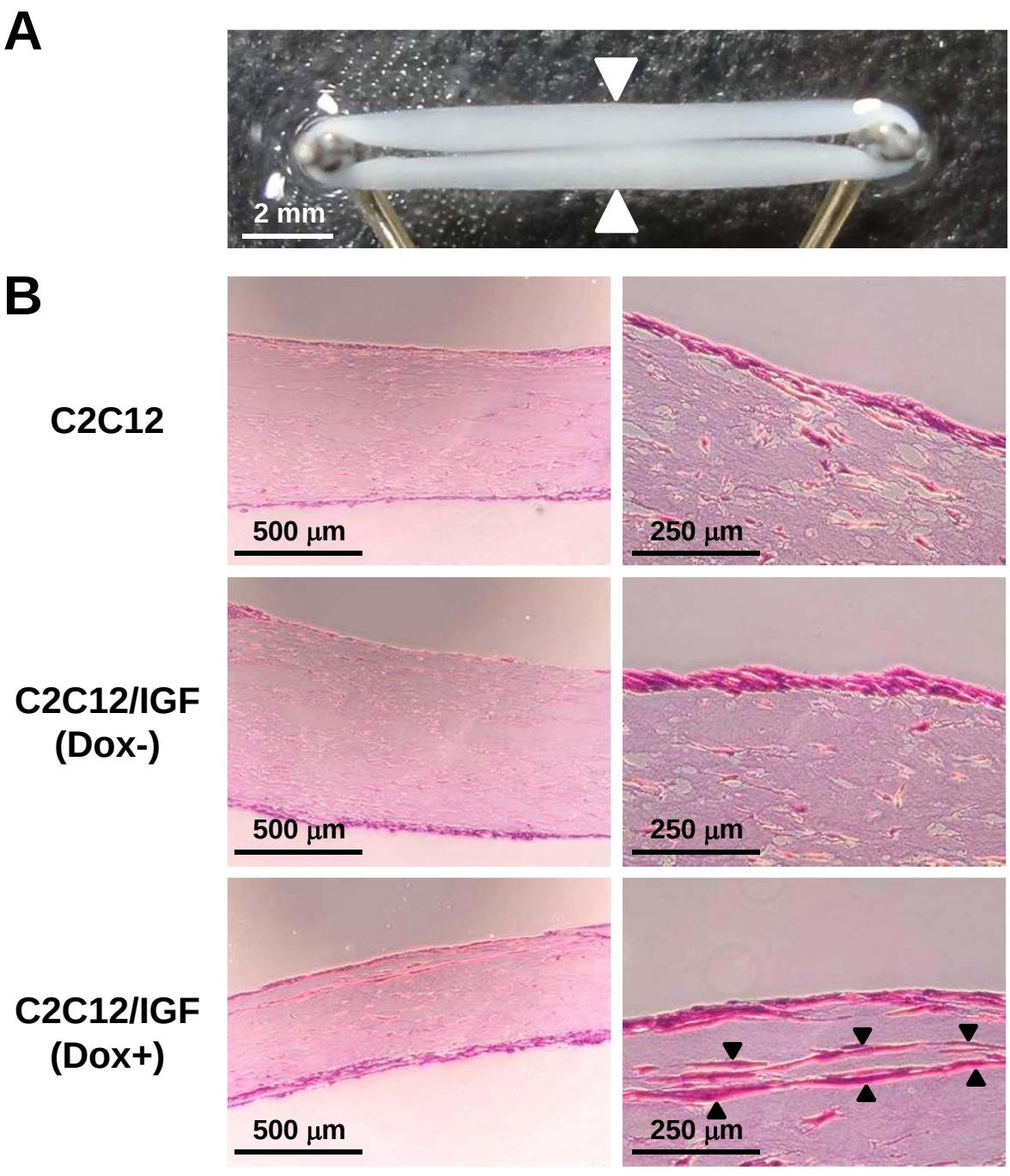

Fig. 4 Sato *et al.*

A

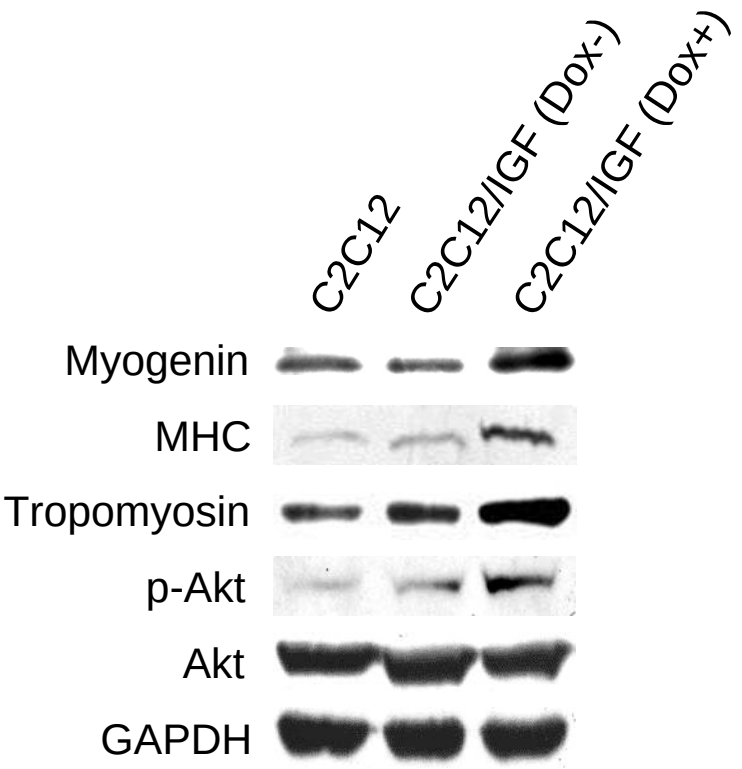

B

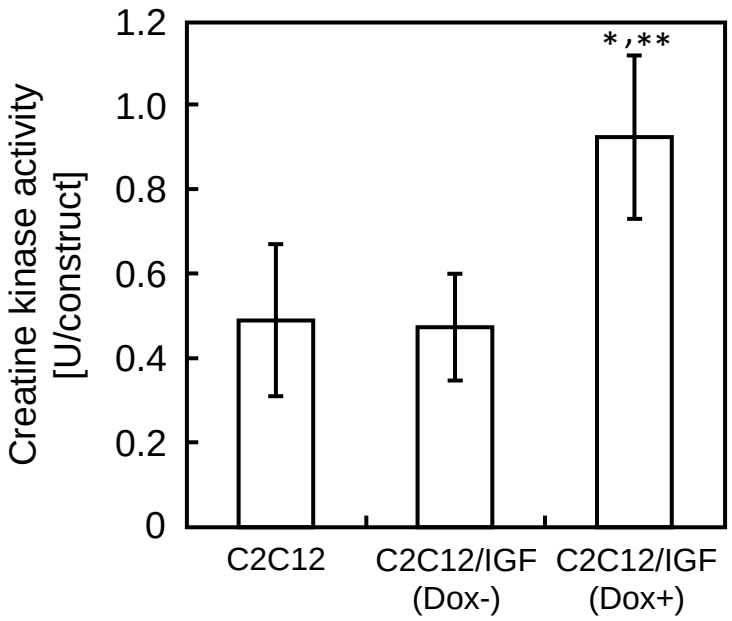

Fig. 5 Sato *et al.*

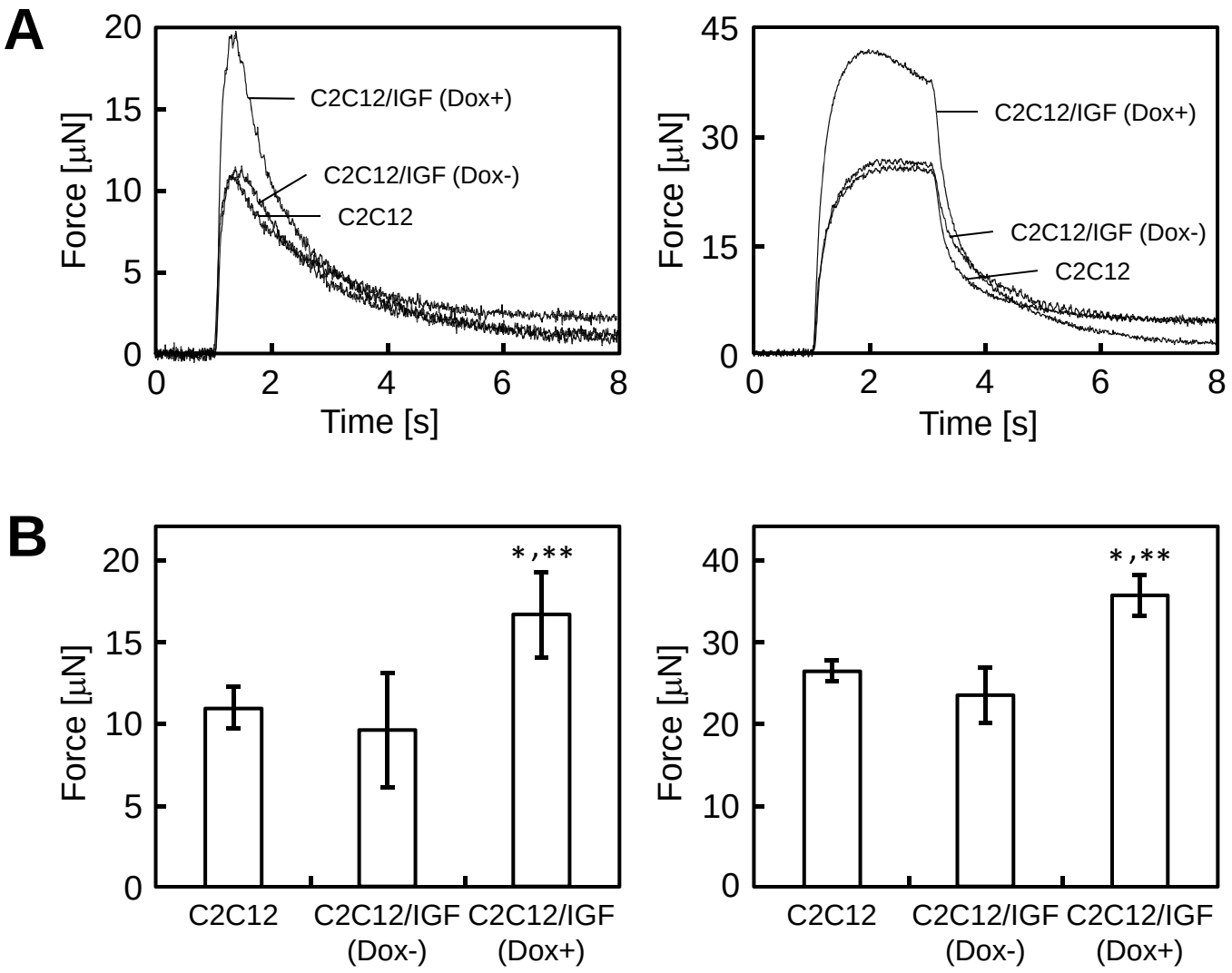

Fig. 6 Sato *et al.*